

BEWEGING EN TRILLINGEN

*Jonas Neeckx
Nicolas Heintz*

Design and dynamics of a cam-follower system

NUMERICAL DATA NR 18

Titularis
Joris De Schutter

A C A D E M I E J A A R 2 0 1 7 - 2 0 1 8

Index

1. Introduction.....	3
• From 45° to 120°: +15 mm	3
• From 120° to 180°: +15 mm	3
• From 200° to 280°: -30 mm	3
2. Definition of the motion law	3
3. Geometry of the follower.....	4
3.1 Undercutting	5
3.2 Pressure Angle.....	5
3.3 Eccentricity	6
3.4 Complete geometry.....	6
4. Rigid-body forces.....	7
4.1 Spring.....	7
4.2 Power.....	9
4.3 Flywheel.....	10
5. Dynamics of a deformable follower	12
5.1 Single rise case.....	12
5.1.1 Conditions.....	12
5.1.2 Numerical solution	13
5.1.3 Approximated solution.....	14
5.2 Multi rise case	14
5.2.1 Numerical solution	14
5.2.2 Analytical solution	15
5.3 Vibration contact force.....	18
6. Conclusion	19

1. Introduction

In this paper a cam-follower system is designed and analysed on dynamic behaviour, both on a rigid-body and a deformable follower. The follower is a translating roller follower, the cam is radial. A spring attached on the follower realises a force-closure.

The following relative motions are necessary:

- From 45° to 120°: +15 mm
- From 120° to 180°: +15 mm
- From 200° to 280°: -30 mm

The motion does not have to start or end at the given angle, but the follower must be at the given positions at that specific angle.

Meanwhile the mechanism needs to be able to provide the following forces:

- From 45° to 120°: a linear ascending pull force from 0N to 300N
- From 120° to 170°: a constant push force of 550N
- From 170° to 240°: constant push force of 300N

The cycle time is 2s. Most of the dimensions in this paper are threshold dimensions to just pass the requirements. For practical use, some safety margins might be advisable.

2. Definition of the motion law

At first it is necessary to choose a certain motion law to obtain the highest level of continuity possible. With this in the mind, the following motion law has been chosen with 0mm at the base circle:

- From 0° to 60°: a dwell at 0mm
- From 60° to 120°: a lift from 0mm to 15mm with half-cycloid C1
- From 120° to 180°: a lift from 15mm to 30mm with half-cycloid C2
- From 180° to 200°: a dwell at 30mm
- From 200° to 280°: a descend from 30mm to 0mm with cycloid C6
- From 280° to 360°: a dwell at 0mm

The first lift only starts at 60° to create a complete cycloid from 60° to 180°. That way there is no sudden jump in the end and start velocity at the transition between both half-cycloids.

The results of the motion law can be seen in figure 1.

As depicted, the cam is continuous until the third order, the acceleration. This is the maximal continuity that can be obtained with a cycloidal motion law. The maximal acceleration is $0.0295 \frac{mm}{degree^2}$. With a cycle time of 2s,

this results in a maximal linear acceleration of $0.0295 \frac{mm}{degree^2} * \left(180 \frac{degree}{s}\right)^2 = 955.8 \frac{mm}{s^2}$

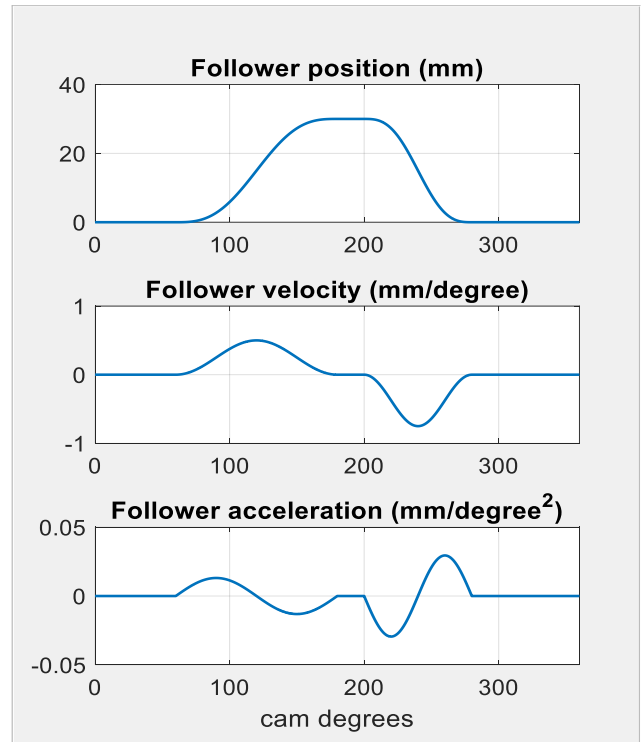


Figure 1: Motion law

3. Geometry of the follower

It is also necessary to know the radius of the follower and base circle when designing a cam-follower system. They have an important influence on both the pressure angle and the appearance of undercutting. Apart from the radii, it is also possible to give the cam a certain excentricity, what enables the possibility to balance the pressure angle.

The ratio L/R_0 can be determined by using the monograms of Kloomok and Muffley based on the maximum angle pressure and the angular difference between start and finish of a segment. Based on this ratio the pitch curve radius is calculated for each segment. To prevent undercutting the highest value is chosen. Table 1 shows the used values.

Table 1: Pitch curve radius

Segment	Angular difference [°]	Rise L [mm]	L/R0 [-]	R0 [mm]
1	60	0	/	/
2	60	15	0,36	41,67
3	60	15	0,36	41,67
4	20	0	/	/
5	80	30	0,5	61
6	80	0	/	/

The restricting segment is segment 5, with $\frac{L}{R_0} = 0.5$. Using a matlab script, the figures of Kloomok and Muffley are generated for a pitch curve radius of 61 mm. Based on these figures the minimum radius of the pitch curve is determined to be 43 mm. The restricting part is the descend from 30mm to 0mm over 80° with cycloid C6.

The radius of the roller follower should be smaller than the pitch curve radius to prevent undercutting. The radius of the roller follower is chosen to be 42mm, which gives a base radius of 19 mm. It is better to keep the radius of the follower quite large, as it ensures a good contact between follower and cam.

3.1 Undercutting

The results of the section above are verified with Matcam. Figure 3 shows the radius of curvature. This figure should never go below zero to prevent undercutting, the peak values can be ignored. As shown by the lowest value on the figure, the graph never reaches zero. As it does approach close to zero, a rather pointy part is expected on the cam. Once the materials are chosen, further examination is needed to ensure this spot can handle the high tensions due to low contact area.

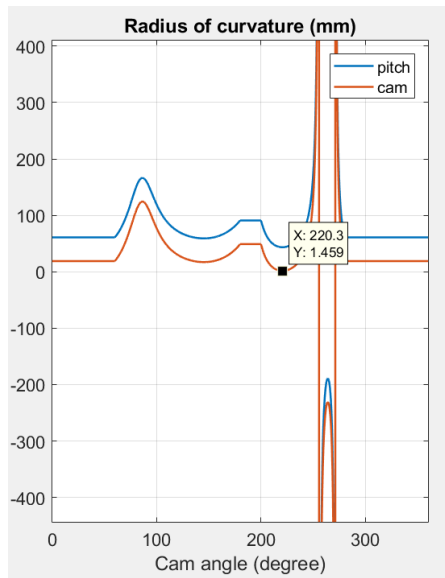


Figure 3: Radius of curvature

3.2 Pressure Angle

Next the pressure angle must be checked. As said before, the pressure angle should never be higher than 30 degrees. Figure 4 shows the pressure angle which is just within the allowed limits.

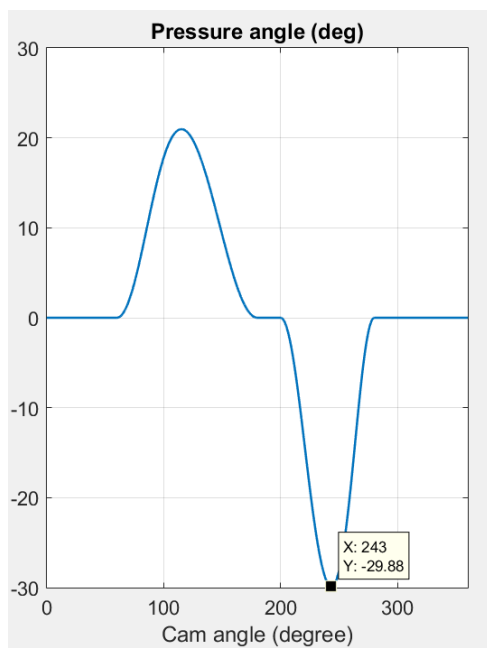


Figure 4: Pressure angle

3.3 Excentricity

At last the maximal pressure angle can be lowered by applying excentricity on the cam. Excentricity merely shifts the pressure angle: if it lowers the pressure angle in the inward motion, it raises the pressure angle during the outward motion. The value of the optimal excentricity has been iteratively calculated by the computer with the aim to minimize the maximal absolute value of the pressure angle $|\alpha|$. The pressure angle is related to the excentricity with the following formula:

$$\alpha = \arctan\left(\frac{f'(\theta) - e}{\sqrt{R_0^2 - e^2} + f(\theta)}\right)$$

It is important to notice that at optimal excentricity, the minimal and maximal pressure angle have the same absolute value. This shows that excentricity merely balances the pressure angle for inward and outward motion.

The optimal excentricity is -7.04mm. At this given excentricity, the pressure angle and radius of curvature can be seen in respectively figure 5 and 6. The radius of curvature is still strictly non-zero and the pressure angle is perfectly balanced. It does become negative, but by reaching a perfectly flat surface with an infinity radius. It never passes through 0.

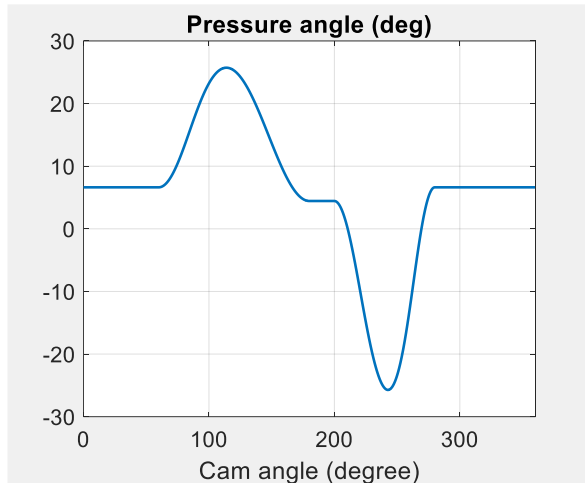


Figure 5: Pressure angle with excentricity

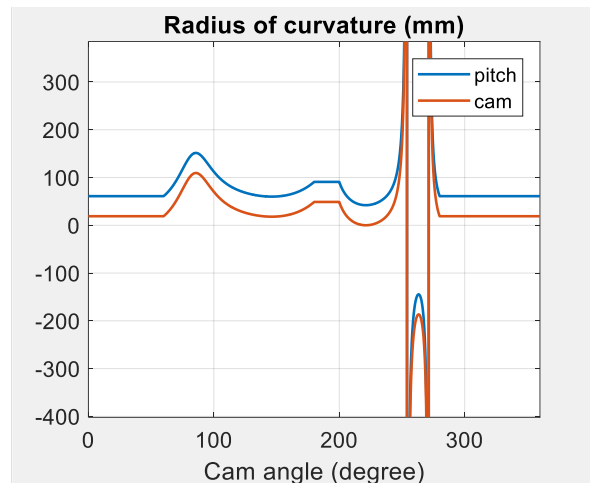


Figure 6: Radius of curvature with excentricity

3.4 Complete geometry

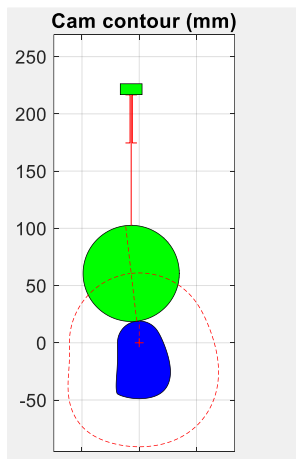


Figure 7: The complete geometry

The entire cam and follower geometry can be seen in figure 7. As calculated, there is a certain point where the radius of curvature reaches close to 0 and a certain point where the cam becomes first flat and subsequently concave. The follower is substantially larger than the cam, but no undercutting takes place. The parameters are summarised in table 2.

Table 2: The cam geometry

R_0	61 mm
R_f	42 mm
e	-7.04 mm

4. Rigid-body forces

4.1 Spring

Once the geometry has been defined, it is possible to analyse the forces on the cam and follower. In this section, the follower and cam are designed as rigid bodies. Only the inertial forces, the force of the spring and external forces are taken into account.

At first a proportional spring must be designed that ensures the contact between the follower and the cam. This spring has both a stiffness $k \left[\frac{N}{mm} \right]$ and a prestress $F_{v0} [N]$. These have to be designed in order to keep the forces as low as possible, but also to make sure that the total force on the follower is always positive.

The Matlab function *spring.m* calculates these parameters by iterating over both the prestress and stiffness. With the used parameters, the normal force on the cam is calculated. If the minimal normal force $N_{min} > 0$ and the maximal normal force is the smallest of all parameters for which $N_{min} > 0$, that set of stiffness and prestress is chosen. In some cases, N_{max} is identical for two sets of parameters. In that case, the set with the lowest average force is preferred.

The normal force is calculated as following:

$$N = \frac{F_{load} + F_{inert} + F_{v0} + k * S}{\cos(\alpha)}$$

With S the lift [mm], α the pressure angle [rad], F_{inert} the inertial force [N] and F_{load} the load applied on the mechanism [N].

The optimal stiffness is 2.84 N/mm, with a prestress of 257,4N. As figure 8 shows, the force is strictly positive. Some iterations also confirmed that this setting is optimal. Due to the low rotational speed, the inertial forces stay very low.

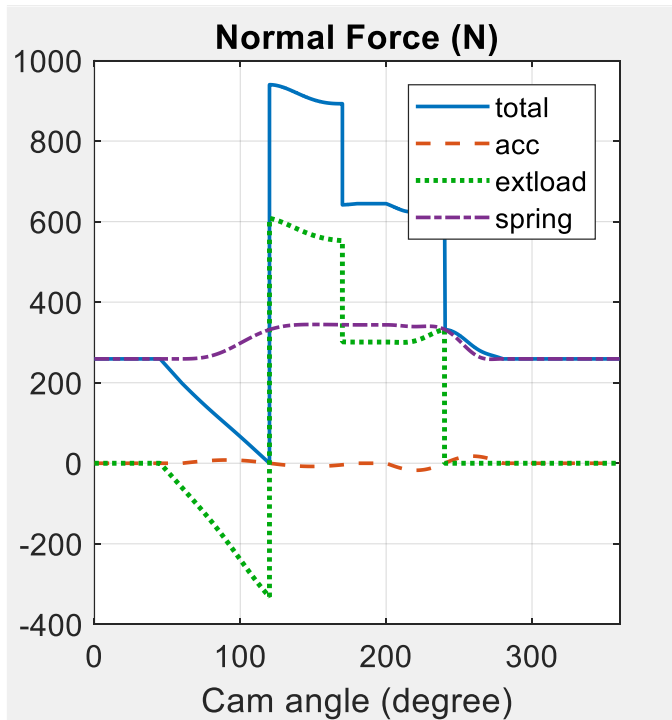


Figure 8: Normal forces on the cam

However, if a new setting requests to double the speed of the cam, the inertial forces are strongly affected. The motion law fixed the acceleration α_θ as mm/degree². However, the inertial force is calculated according to Newton's second law: $F = m * a = m * \alpha_\theta * \omega^2 * 10^{-3} \sim \omega^2$. If the rotational speed doubles, the inertial force multiplies by four. This effect can be seen on figure 9. As the acceleration was just 0 at the critical point, the same spring can be used. However, a more optimal configuration is obtained with $k = 5.24 \frac{N}{mm}$ and $F_{v0} = 221.4N$. This configuration is shown in figure 10.

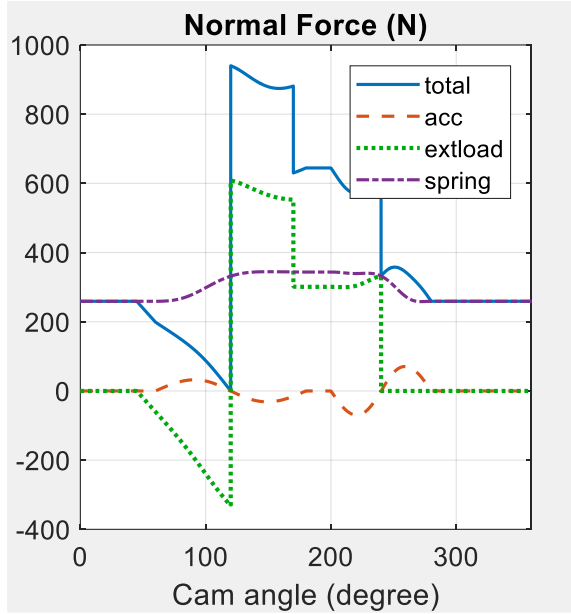


Figure 9: Normal forces at double speed with identical spring

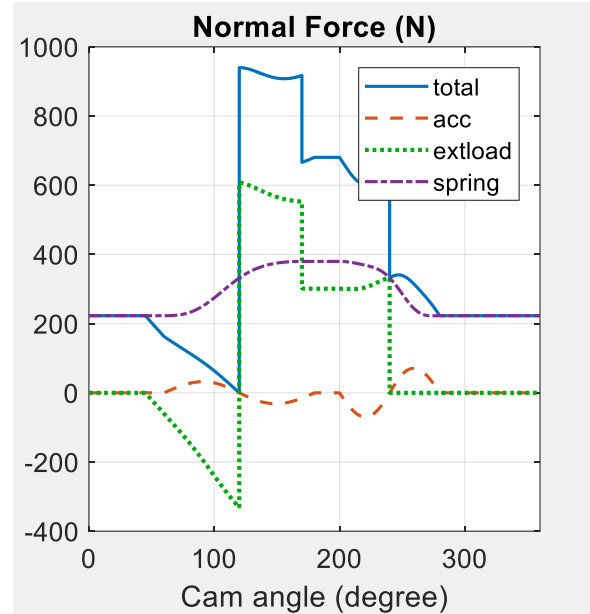
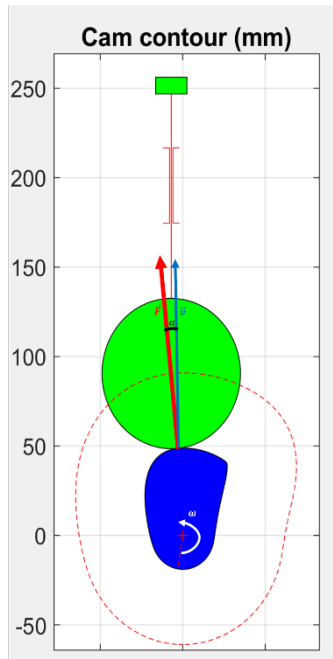


Figure 10: Normal forces at double speed with new spring

4.2 Power



When designing the motor used to power the cam, both the instantaneous and average power are very important parameters. As the follower strictly moves up and down, the easiest way to calculate the instantaneous power is

$$P = \vec{F} \cdot \vec{v} = N_{tot} * \cos(\alpha) * V * \omega * 10^{-3}$$

With N_{tot} [N] the total normal force exerted on the cam, α [rad] the pressure angle, V [mm/rad] the lift per radial, ω [rad/s] the angular speed. The direction of \vec{F} , \vec{v} and ω are drawn on figure 11.

Due to the scalar product and a strictly vertical movement of the follower, only the vertical forces influence the power. The total force applied on the follower contains the inertial force, the spring force and the external force, all forces are independent of the cam's geometry if the spring, the followers mass and the motion law stay identical. Thus, there is no expected difference between the instantaneous power of a cam with or without excentricity.

Figure 11: Force and speed on the follower

The result of the instantaneous power can be seen in figure 12. As expected, the instantaneous power with and without excentricity is identical.

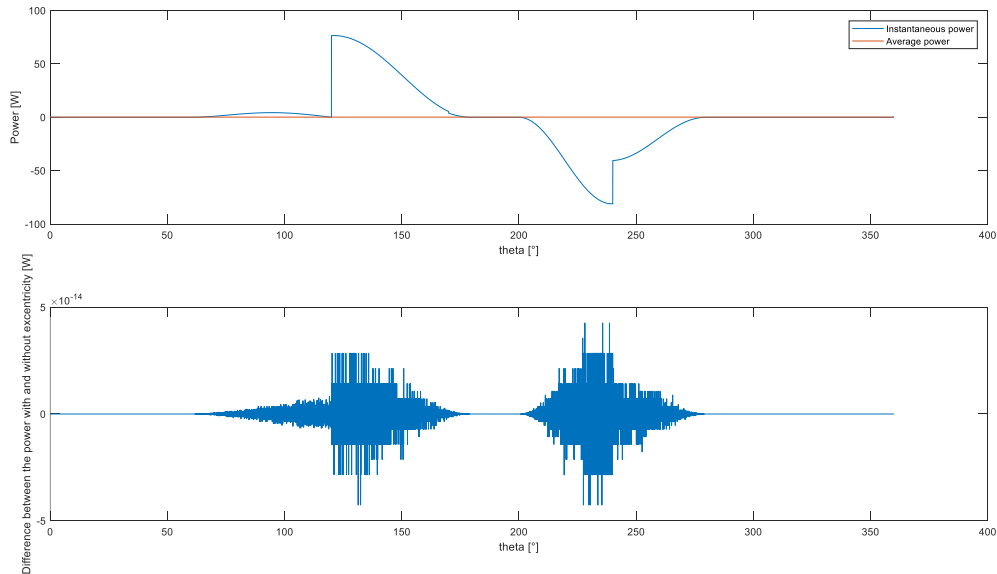


Figure 12: Power and control of the mechanism

The average power is only 0.1466W. This means that the mechanism requires more power than it delivers. However, the low value hints that the mechanism is almost self-sufficient. This allows the system to be driven by a very cheap motor. Energy loss due to friction has not been considered.

4.3 Flywheel

As $P = T * \omega$, the torque is easily calculated from the power. The average torque is 0.0467Nm and can be seen next to the instantaneous torque in figure 13.

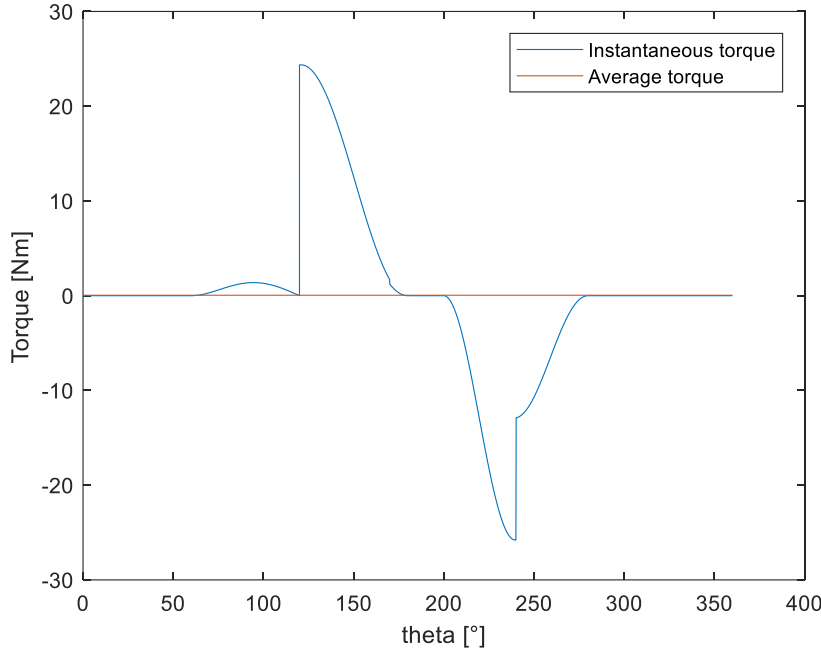


Figure 13: The instantaneous and average torque

Even though the low average torque permits a cheap motor, the high pikes in torque demand could lead to a large speed variation, which is unwanted. The motor is only supposed to deliver its nominal torque, which equals the average torque. When the motor cannot deliver the demanded torque, the mechanism slows down. In order to keep the relative deceleration and acceleration below 5% with respect to the nominal rotational speed, a flywheel is installed.

In the process of calculating the inertia, the first step is to find the place where the rotational speed is maximal and minimal. In this case the needed torque only rises above the average torque between 63.6° and 178.1° . Inside this domain, the cam decelerates, outside this domain it accelerates. The maximal speed is thus obtained at 63.6° , the minimal speed at 178.1° . The loss in speed can be calculated as following:

$$A_{max} = \int_{\theta_m}^{\theta_M} T(\theta) - T_{av} d\theta = \frac{1}{2} * I(\omega_M^2 - \omega_m^2)$$

$$\omega_{av} \approx \frac{\omega_M + \omega_m}{2}$$

$$K = \frac{\omega_M - \omega_m}{\omega_{av}}$$

$$I = \frac{A_{max}}{K * \omega_{av}^2}$$

From the torque and the two angles, A_{max} has been calculated as 13.7Nm. ω_{av} is the required π rad/s. ω_M and ω_m may only vary with 5% with respect to ω_{av} . As the top speed and lowest speed

are not necessary at the same relative distance from ω_{av} , $K = 0.06$ has been chosen as safety for the inaccurate approximation of ω_{av} .

The chosen parameters result in $I = 23.1 \text{ kgm}^2$. If a cylindrical steel flywheel ($\rho = 8000 \frac{\text{kg}}{\text{m}^3}$) were designed, a possible dimension would be a flywheel with a diameter of 0.6m and 0.227m long. This would be bigger than the entire mechanism itself. This high moment of inertia can be explained by the high peaks in torque, the low average torque and the fact that all deceleration happens in one domain. If the deceleration and acceleration would alternate more, a lower value for A_{max} would be calculated.

This value can also be estimated from figure 13: the total area above the average torque can be approximated by two triangles. The first is about $\frac{\pi}{3}$ radians long and 1 Nm high. The second one is also about $\frac{\pi}{3}$ radians long and 25 Nm high. The total area is thus 13.6 Nm, almost exactly equal to the A_{max} that was previously calculated. This estimation gives an $I = 23.0 \text{ kgm}^2$. This close estimation suggests that the calculation is probably correct for the given torque.

In figure 14 the evolution of the rotational speed can be seen in both absolute as relative values. The safety in the K-factor is indeed needed as the cam rotates most of the time at a higher speed, but drops in speed during a third of his cycle. The maximal speed stays below 1.02 times the average speed, the minimal speed stays above 0.95 times the average speed.

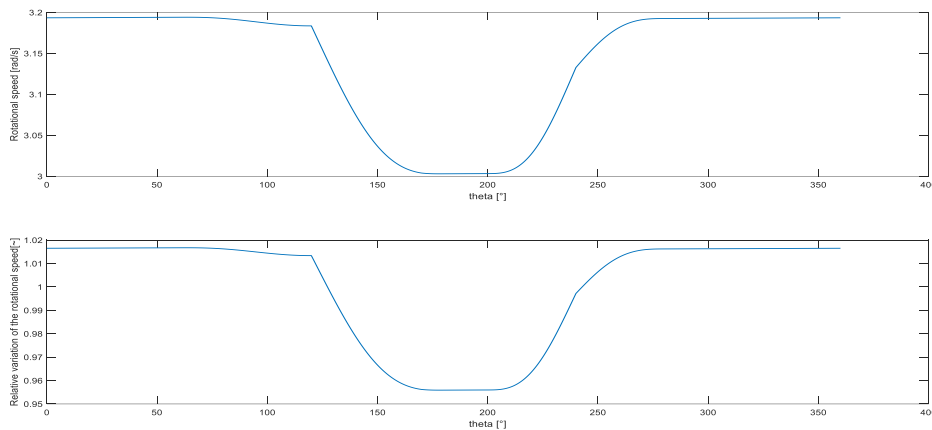


Figure 14: Variation of the rotational speed

During the start-up, the cam must accelerate as well. Due to the high moment of inertia, this effect cannot be ignored. Start-up usually goes together with high peak currents through the motor. Even though the nominal torque of a motor is fixed, it can produce higher torques for a short period of time. The torque needed for start-up is determined by the angular acceleration:

$$T - T_{load} = I * \alpha$$

Even though a motor can produce higher torques, it also has a limit, as its wires might burn when the applied current exceeds a certain point. If possible, it might be a lot cheaper to start slowly, so the motor doesn't have to handle very high currents.

The maximal torque of a motor is also dependant of the speed. In order to start accelerating, the torque at $0 \frac{\text{rad}}{\text{s}}$ must be higher than the instantaneous load. This can be very high if the pressure angle and external load at the given position is high. An external assist might be needed to get cam in a position with a lower load.

5. Dynamics of a deformable follower

5.1 Single rise case

5.1.1 Conditions

The single rise case is used on one movement followed by a period of dwell. It can only be used if the transient response has died out before the next rise/return. There can only be one degree of freedom, the spring force must maintain the contact between the cam and the bottom of the follower at all time and can not affect the contact force between cam and follower.

Any functional forces acting on the cam-follower, gravity and nonlinear friction are neglected. First a numerical solution is suggested, then an approximate solution is compared to the numerical solution in a fast way. The analytical solution is not discussed in this paper.

The approximate solution is only viable for certain values of λ and ζ and the homogeneous part of the forced response must be completely died out at $\tau = 1$. The given trajectory is then replaced by:

$$\theta(\tau) = \frac{Q(\tau - 1)^N}{N!} + 1$$

To achieve a 10% accuracy on the difference between the exact and approximate magnitude of the exponential envelope $\lambda * \zeta$ should be bigger than 0.75.

The most critical segment will be the segment with the largest acceleration and followed by a dwell. In this case this is segment five with a rise of -30 mm over 80 degrees, followed by a 140 degrees long dwell. This segment also has the biggest displacement per degree of 0.375 mm/°.

The equivalent structural follower stiffness can be determined by

$$k_f \geq m \left(\frac{0.75 * 2\pi}{\zeta t_1} \right)^2 - k_s :$$

The condition $\lambda * \zeta > 0.75$ is used in this equation. This gives an equivalent structural follower stiffness of $1,9712 * 10^5 \text{ N/m}$. The condition that the transient response must be died out by the next rise/return ($\tau = 2,75$) is also met:

$$e^{-\zeta * 2 * \pi * \lambda * (\tau - 1)} = 0.00026$$

5.1.2 Numerical solution

A numerical analysis is done using the Matlab command `lsim`. The following system is used:

$$\frac{\Gamma(s)}{\Theta(s)} = \frac{(2\pi\lambda)^2}{s^2 + 2\zeta(2\pi\lambda)s + (2\pi\lambda)^2}$$

The input used is the exact input generated by Matcam. The time and the rise of the system are made dimensionless after which the system is solved. In figure 15 the input, the output and the difference between them is shown. An initial vibration with an amplitude of 10^{-3} which dies out after a while can be seen. The free response starting from $\tau = 1$ is also clearly visible.

The amplitude of the exponential envelope at $\tau = 1$ is calculated as well. This value will be useful to make a comparison between the numerical and the approximated solution. The complete calculation and formulas used can be found in the Matlab files and the course material.

$$A_1 = 3.8947 * 10^{-4}$$

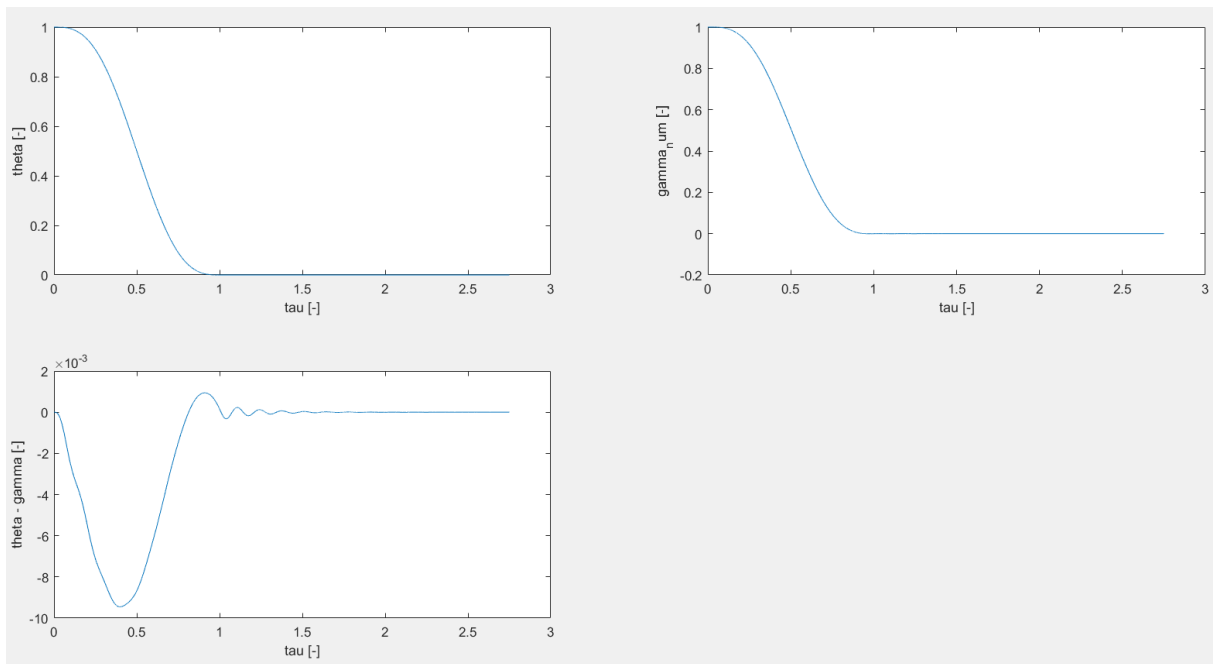


Figure 15: Dimensionless input, output and difference in function of τ

5.1.3 Approximated solution

The conditions for the approximated solution are given in section 5.1.1. The response is predicted without determining the forced part of the response.

To make a quick check between the numerical and approximated solution the amplitude of the exponential envelope of the approximated solution is calculated.

$$\tilde{A}_1(Q, N, \lambda, \zeta) \approx \frac{Q}{(2\pi\lambda)^N}$$

Because we are working with cycloidal motions, $N = 3$ and $Q = (2 * \pi)^2$. The amplitude is now equal to $3.7916 * 10^{-4}$.

Next the accuracy of the approximate solution is determined.

$$\varepsilon = \left| \frac{A_1 - \tilde{A}_1}{A_1} \right| = 0.0265$$

The difference is below 10%, which means the approximate solution can be assumed correct.

5.2 Multi rise case

Instead of just looking at the most critical segment, the multi rise case looks at the entire cam. The multi rise case is first determined in two ways, an analytical and a numerical way. After comparing these, the multi rise case is compared to the single rise case in the most critical segment.

5.2.1 Numerical solution

In the same way as the single rise case, the numerical solution is calculated using the Matlab command `lsim`. The result is shown in figure 16. The shape of the figure seems correct. A more in-depth discussion will be done after the analytical calculations.

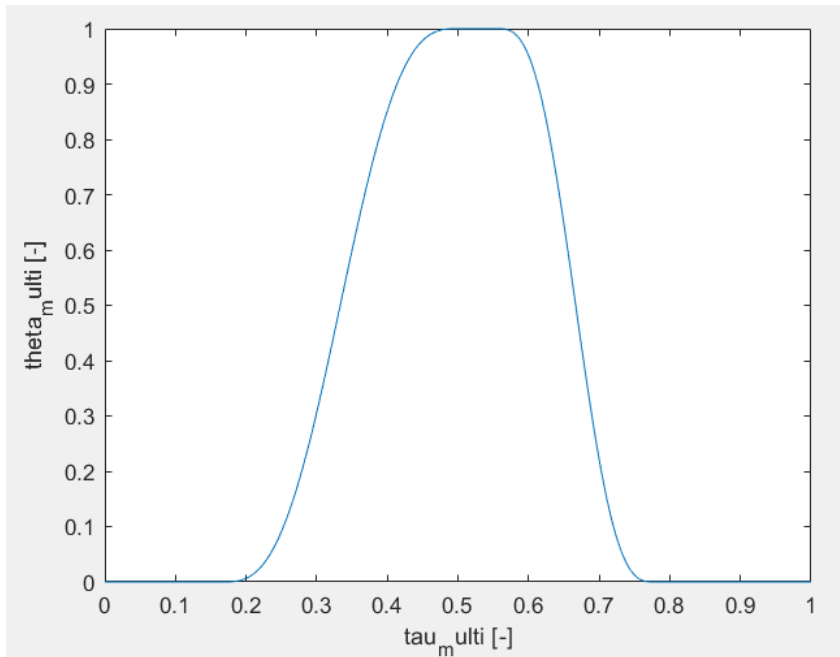


Figure 16: The dimensionless input against the dimensionless angular time

5.2.2 Analytical solution

A frequency domain analysis can be done by expressing the known input motion as a Fourier series. 100 harmonics are chosen to approximate the input in a reasonably accurate manner. The homogeneous part of the solution is not considered because it has died out in steady state. To calculate the Fourier series, two Matlab scripts are downloaded from mathworks. These scripts are also added to the Matlab files. We refer to the Matlab code for the calculations.

Figure 17 shows the output of the analytical solution, we can see that it has the right shape.

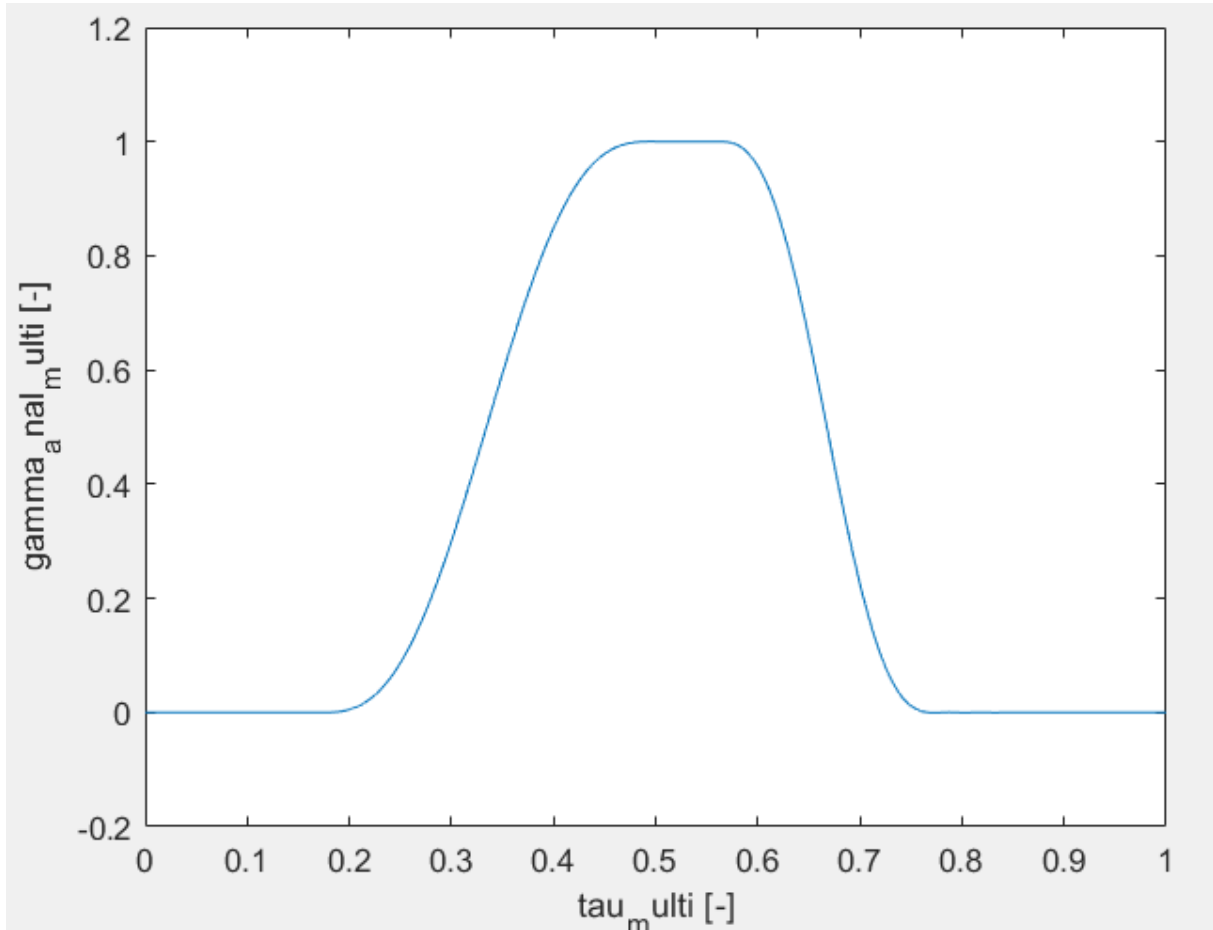


Figure 17: Output of the analytical analysis against the dimensionless angular time

Figure 18 shows the difference between the output of the numerical and the analytical solution. The biggest errors are found in the middle of the rise of the segments, at 120 degrees because half cycloids 2 and 1 form one smooth motion, and at 240 degrees, the middle of segment five in which we go from 30 mm to 0 mm.

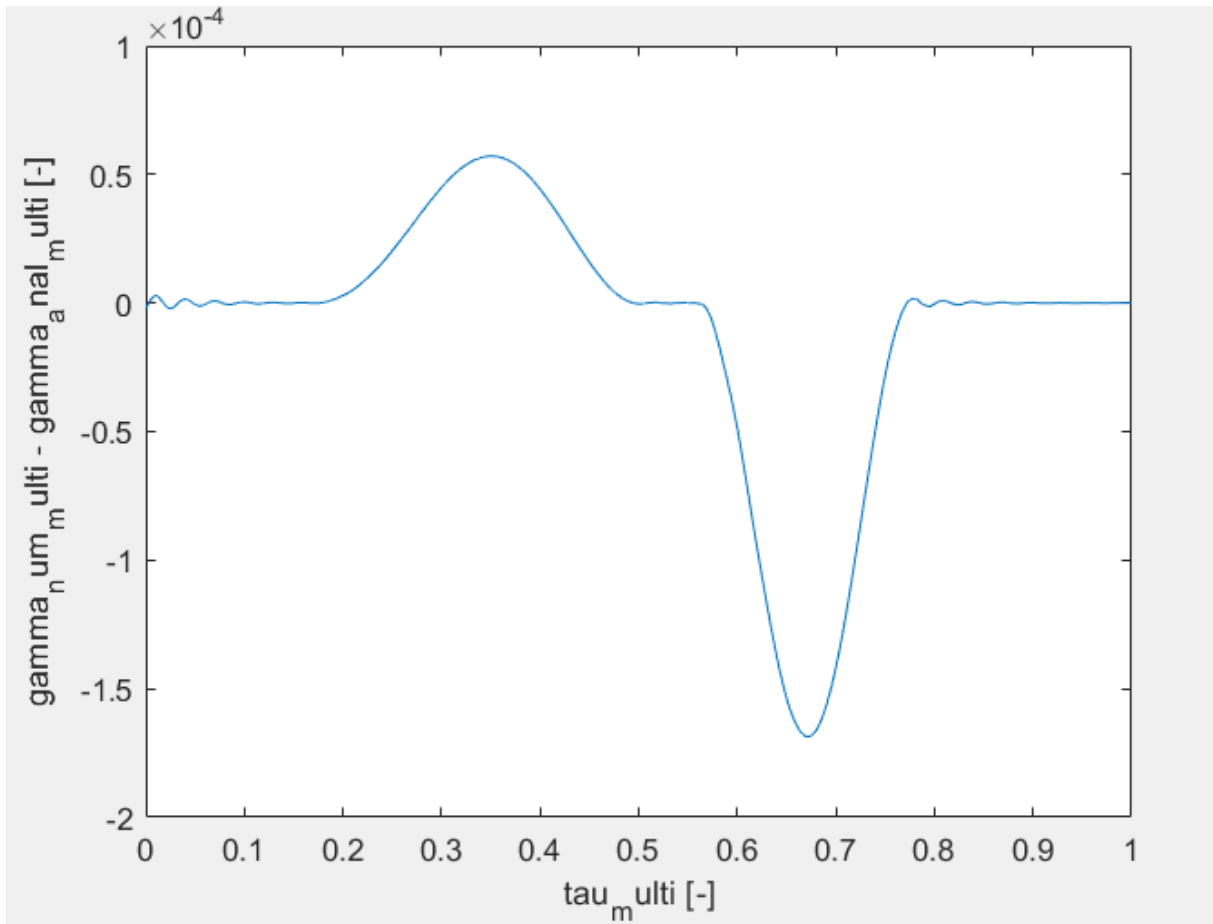


Figure 18: Difference in output between the numerical and analytical analysis

Figure 19 shows the difference in input and output for the numerical and the analytical solution. We can see that both graphs have the same shape but the vibrations are smaller for the numerical solution than the analytical solution. The error can be seen on figure 18.

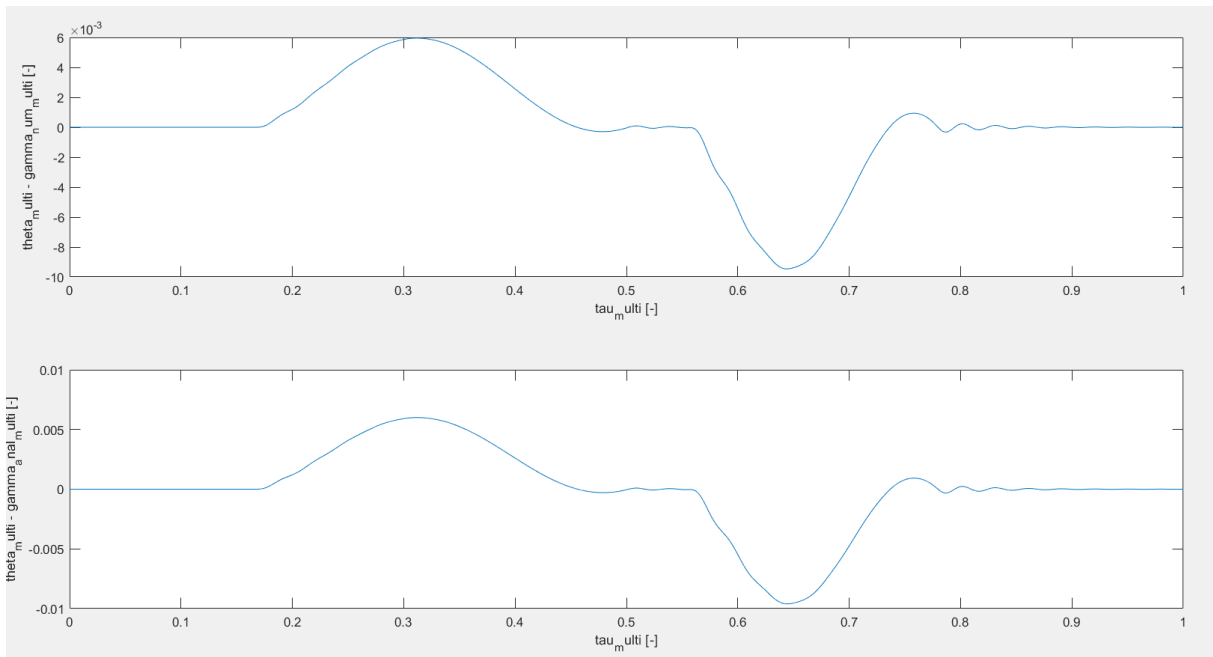


Figure 19: Difference in input and output for the numerical and the analytical solution

Figure 20 shows the difference between the single rise case and the multi rise case. The difference between the inputs is equal to the machine accuracy of Matlab. The difference between the last two graphs is the error of figure 18. The initial vibration in the graphs can be explained by the transient behaviour of the multi rise solution because of the initial vibrations caused by the previous segment. The single rise case doesn't have previous segments, so it doesn't have the same transient behaviour. As expected the difference dies out after τ equals 1.

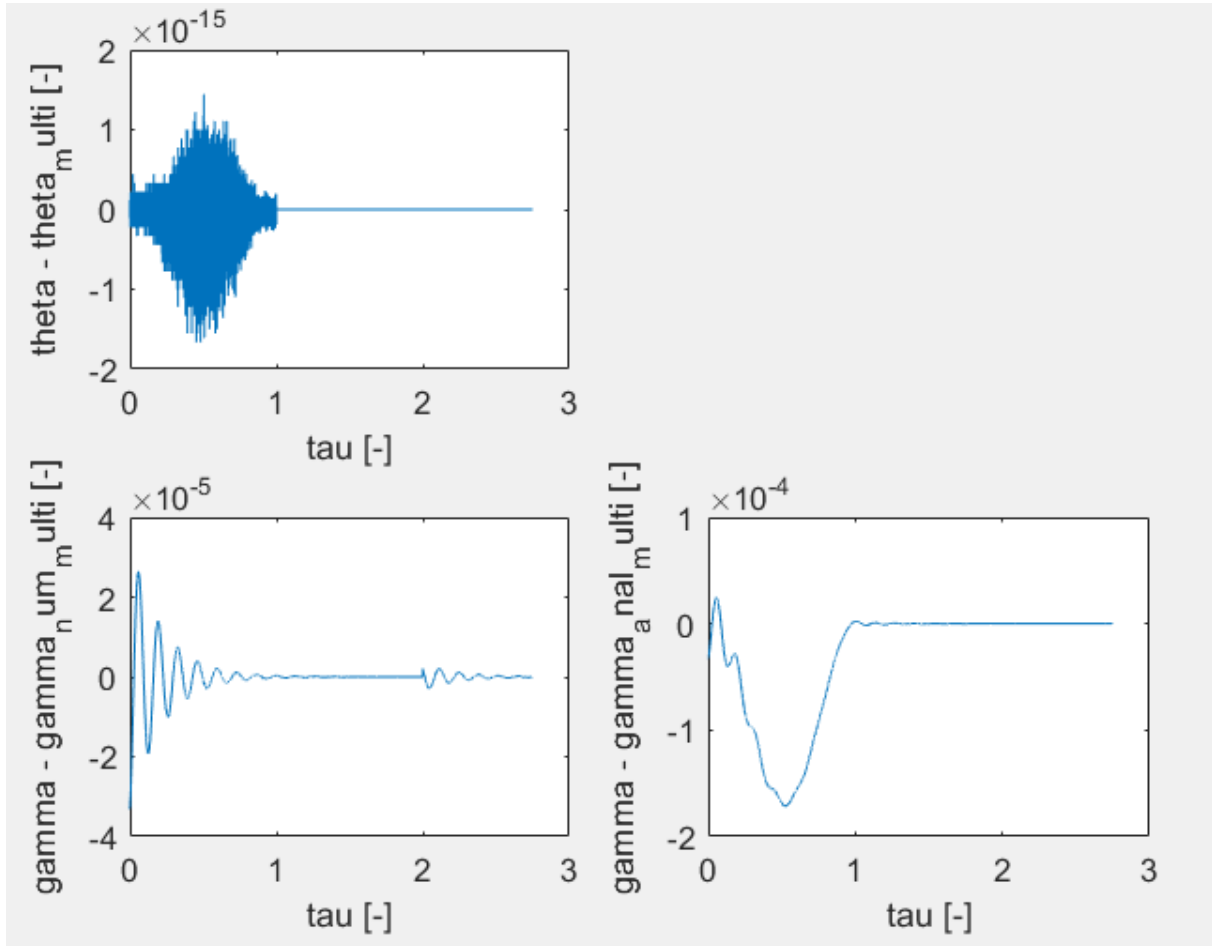


Figure 20: Single rise and multi rise comparison

5.3 Vibration contact force

There will be additional contact forces because of the follower. These forces can be calculated as

$$F = h * k_f * (y(t) - u(t)) / \cos(\alpha)$$

The cosine of the pressure angle is needed to get the normal force.

Figure 21 shows the additional contact force.

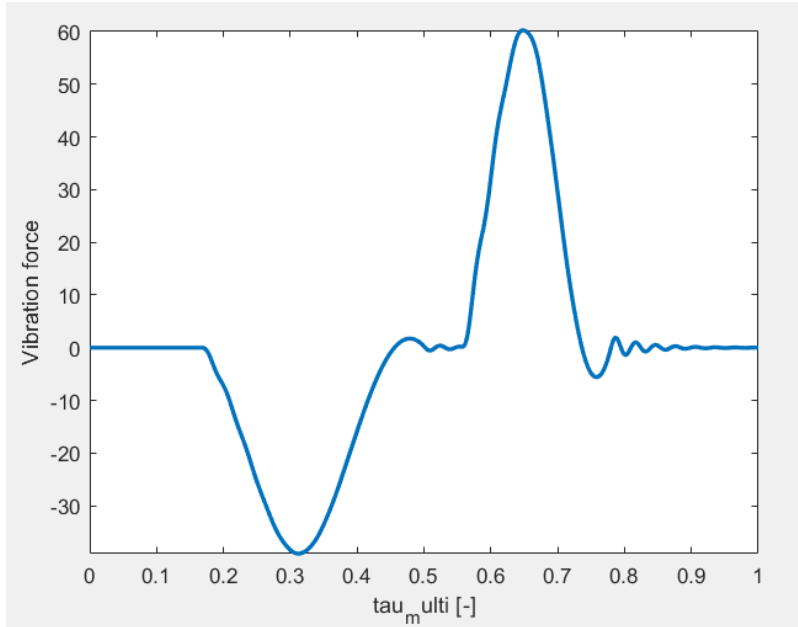


Figure 21: resulting force between follower and cam

Figure 22 shows the new total contact force. The total contact force becomes smaller than 0N with a minimum of -37.2714N which means the stiffness k_s must be adjusted to prevent any loss of contact or a prestress of 38N can be added to the spring.

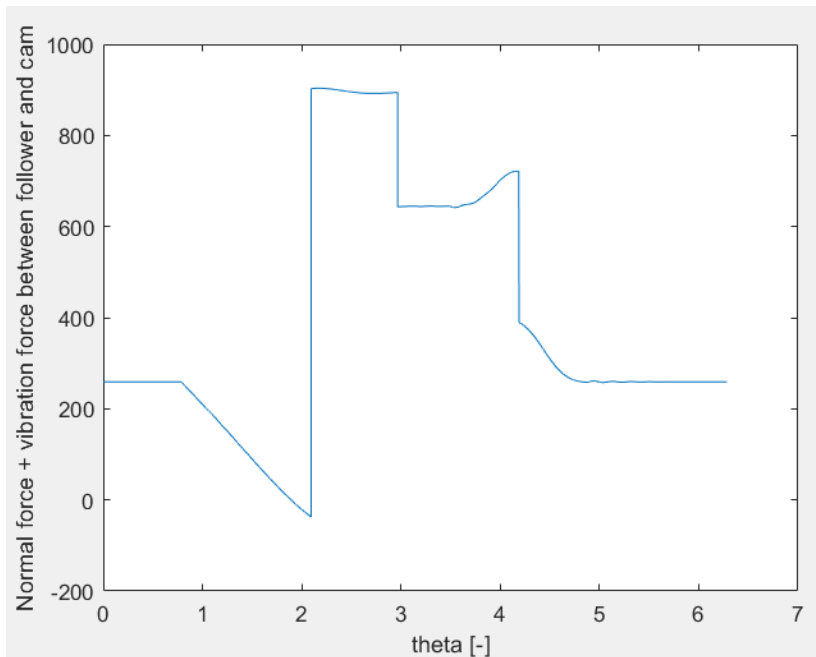


Figure 22: Total contact force

6. Conclusion

At first a motion law has been established for minimal acceleration. Subsequently the geometry has been defined. While defining the geometry, there has been paid attention to keep the pressure angle below 30° and to prevent undercutting. In order to minimise the pressure angle, an optimal excentricity has been calculated.

With the obtained geometry a first analysis of the forces using a rigid-body model has been done. In this analysis a spring has been designed that ensures continuous contact between cam and follower, but keeps the normal forces on the cam to a minimum. There has also been a power analysis in order to design the motor. From the given power, the torque on the cam has been calculated.

Once the instantaneous torque and average torque was known, a flywheel has been designed that keeps the variation in speed below 5% compared to the average speed.

As a rigid body is only an approximation of the reality, a second force analysis has been done with a deformable body. At first the analysis on the worst case single rise has been done, followed by the analysis of a multiple rise body in steady state. Both models are calculated analytically and numerically as a control. From the forces obtained by this analysis we could conclude that a higher stiffness or prestress was needed for the spring in order to ensure contact between cam and follower.

All calculations are controlled when possible and all controls passed.